

Date of publication xxxx 00, 0000, date of current version xxxx 00, 0000.

Digital Object Identifier 10.1109/ACCESS.2017.DOI

Impact of Optimal Control of Distributed Generation Converters in Smart Transformer Based Meshed Hybrid Distribution Network

CHANDAN KUMAR¹, (SENIOR MEMBER, IEEE), RAMPPELLI MANOJKUMAR², (STUDENT MEMBER, IEEE), SANJIB GANGULY³, (SENIOR MEMBER, IEEE) AND MARCO LISERRE⁴, (FELLOW, IEEE)

^{1,2,3}Electronics and Electrical Engineering, IIT Guwahati, Guwahati, India (e-mail: chandank@iitg.ac.in, manoj023manoj@gmail.com, sanjib191@gmail.com)

⁴Chair of Power Electronics, Faculty of Engineering, Christian-Albrechts-University of Kiel, Germany. (e-mail: ml@tf.uni-kiel.de)

Corresponding author: Chandan Kumar (e-mail: chandank@iitg.ac.in).

"This work was supported in part by the Science and Engineering Research Board (SERB), Department of Science and Technology, India, under the Research Grant ECR/2017/001564 and in part by Central Power Research Institute (CPRI), India research project entitled "Design, operation, and control of distributed generation (DG) integrated unified power quality conditioner (UPQC)" in electric grid"

ABSTRACT A smart transformer (ST) based meshed hybrid distribution network is realized by extending ST low voltage dc (LVDC) link to form a LVDC line which connects dc buses of existing distributed generation (DG) converters. This paper proposes a method for optimal operation in such ST based meshed hybrid distribution network. A CIGRE LV residential distribution network with DG sources is connected at ST low voltage ac (LVAC) and LVDC terminals. All the DG sources are proposed to be connected at LVDC line. The power management scheme and method of determining power flow solution for the considered distribution network are proposed. An optimal problem is formulated for determining the active and reactive power references of DG converters while maintaining the load bus voltages within the grid limits and considering the DG converters constraints. The minimization of energy drawn from ST medium voltage (STMV) grid is considered as objective function and solved using genetic algorithm. To know the impact of proposed optimal control DG converters various performance indicators i.e., energy loss, operating energy costs, voltage profile and sizing of ST converters are considered and compared with existing literature.

INDEX TERMS Distributed generation converters, meshed hybrid distribution network, smart transformer.

Nomenclature

A. Notations

dp	Death penalty	$P_{dgc}\{Q_{dgc}\}$	Active {reactive} power of DG converter
E_{grid-d}	MVAC grid demand	$P_{lbac}\{P_{lbdc}\}$	Load bus power in LVAC {LVDC} network
E_{mvac}	MVAC grid energy	$P_{lvc-wcs}\{Q_{lvc-wcs}\}$	ST LV converter active {reactive} power in worst case scenario
EL	Energy loss	$P_{lvc}\{Q_{lvc}\}$	Active {reactive} power supplied by ST LV converter
EP	Energy price	$P_l\{P_{dg}\}$	Load {DG source} power
$n_l\{n_{dg}\}$	Number of loads {DG sources}	$P_{mvc-wcs}\{Q_{mvc-wcs}\}$	ST MV converter active {reactive} power in worst case scenario
OC	operating energy cost	$P_{mvc}\{Q_{mvc}\}$	Active {reactive} power supplied by ST MV converter
$P_{ac-loss}\{Q_{ac-loss}\}$	Active {reactive} power losses in ac line	$P_{odgc-ref}\{Q_{odgc-ref}\}$	Optimal active {reactive} power references of DG converters
$P_{dc-loss}$	dc line loss		
$P_{dgc-ref}\{Q_{dgc-ref}\}$	Active {reactive} power references of DG converters		

P_{tl}	Total load power in the system
$pf_{dgc-min}$	Minimum power factor limit of DG converters
pf_{dgc}	Power factor of DG converters
S_{dgc-r}	DG converter kVA rating
$S_{lvc-r}\{S_{mvc-r}\}$	kVA rating of ST LV {MV} converter
T	Total time horizon
t	Time
T_c	Control horizon
V_{ad}	Average voltage deviation
V_l	Load bus voltage
$V_{min}\{V_{max}\}$	Minimum {maximum} bus voltage magnitude limits
V_{ref}	Reference voltage
$V_{wmin}\{V_{wmax}\}$	Worst minimum {maximum} bus voltage magnitude

B. Indices

i	Index of loads
j	Index of DG sources

C. Abbreviations

DG	Distributed Generation
GA	Genetic algorithm
LVAC	Low voltage ac
LVDC	Low voltage dc
MPP	Maximum power point
MVAC	Medium voltage ac
PV	Photovoltaic
ST	Smart Transformer
ToU	Time-of-use

I. INTRODUCTION

The use of distributed generation (DG) is continuously increasing in the low voltage ac (LVAC) distribution grid with the availability of renewable energy sources of photovoltaic (PV) and wind power [1]. However, this increased use of DG sources causes several problems like increase in line losses, reverse power flow, over-voltage, etc., [2]. Moreover, the residential distribution networks experience more power loss due to the resistive nature of distribution lines. This power loss increases the energy drawn from the grid which results in higher operating energy costs. Therefore, it is important to minimize the energy drawn from the grid in residential distribution networks [3]. The power requirement mainly depends on load demand along with the line losses. In case if loads are modelled as constant power loads, the minimization of energy loss is same as that of minimization of energy requirement of distribution network as it is not possible to control the load powers. There are several methods used for reducing energy loss in distribution networks.

The use of capacitor banks [4], DG sources allocation [5], and network reconfiguration [6] are few techniques applied to reduce energy loss. However, the capacitor banks can not be controlled in continuous steps which is a disadvantage

associated with them [7]. The DG sources are also used for the reduction of energy loss with the help of power converters. These power converters play an important role in improving the performance of distribution systems. Based on the control strategy, these power converters are operated in two modes i.e., grid following mode and grid forming mode [8]. The power converters act as ac current sources providing active/reactive powers as per the given references in grid-following mode. The power converters operate as ac voltage sources while maintaining the terminal voltage and frequency as per given references in grid-forming mode [9].

In case of conventional ac grid configuration mainly the reactive power from DG converters is controlled by operating them in grid following-mode. The reactive power control using photovoltaic (PV) inverters for minimizing the energy loss and improving the voltage profile is discussed in [10]. The active power from DG converters is either maintained at a reference of maximum power point power or curtailed. It means the DG converters are underutilized when there is no or less power available from DG sources. Further, the DG sources can be either ac or dc sources (e.g., PV and wind power sources). In this scenario, it is important to have an operating dc system along with the ac system (hybrid ac/dc system). This increases the efficiency, reliability while improving the stability of the system [11]. However, there are several issues with the use of DG sources in hybrid ac/dc systems like power quality problems, reverse power flow and power management, etc. [12].

Smart transformer (ST) is a well-known solution for tackling the aforementioned issues in the distribution network [13], [14]. The ST is a solid state transformer (SST) made up of power electronics converters which has advanced control and communication features. In [15], the architecture and various control schemes of the ST for improving the modern grid performance are discussed. The ST provides the features of conventional power transformer such as isolation and change of voltage level along with the ancillary services like frequency control, load compensation, power flow control and voltage control at the same time etc. [16], [17]. The availability of dc links in ST configuration reduces the required number of converters for dc source connection and the cost of reinforcements of lines [18]. Moreover, it provides the possibility of creating ac/dc hybrid microgrids using ST [19].

A hybrid ac/dc microgrid with the application of SST and centralized energy storage is studied in [20]. A power management and coordination control is proposed to increase the power supply reliability of the SST based hybrid MG. In [21], the ST voltage control capability for reducing the load demand is discussed. The energy costs are reduced while performing the optimal power flow analysis. Further, the operation and control of ST in meshed hybrid systems for various configurations is presented in [22]. The ST can operate in meshed-grid configurations with more flexibility and control. There are several meshed electric grid configurations presented in literature. The ST based meshed grid structure is used in [23] to achieve reduction of the line losses and

improved supply redundancy.

In [24], a meshed hybrid grid configuration is proposed by connecting a dc line between the ST LV dc (LVDC) link and the dc bus of the DG converters. The various benefits associated with the added dc line in the ST based microgrid system are discussed. It is shown that the power loss in the system is reduced with the addition of dc line. Moreover, the improved voltage regulation caused due to the added dc line is discussed. Also, the advantages of meshed hybrid system considering the protection aspects are discussed in detail. It is possible to control both active and reactive powers using the proposed meshed hybrid grid configuration. However, in [24], DG converters are used to supply only active power. The total load power requirement is shared among the DG converters in proportion to their kVA ratings which is not optimal. Moreover, the reactive power control of DG converters is not performed.

To avoid this, both active/reactive powers of DG converters are controlled optimally in [25] for minimizing the energy loss in ST based meshed hybrid distribution network. Genetic algorithm (GA) is used to obtain the optimal results. However, the system analysis is limited to LV converters operation. The operation of ST MV converters is not discussed. Further, the impact of optimal DG converters control considering several operating benefits such as the energy cost analysis, voltage profile and sizing of ST converters is not discussed. To avoid this research gap, the main purpose of the study in this paper is dedicated to the discussion of operation of ST MV converters in ST based meshed hybrid distribution network and presentation of the impact of optimal control of DG converters on energy cost, voltage profile and sizing of ST converters. These are the novel contributions of this paper. In summary, the overall contributions of the paper are as follows.

- 1) To propose the power management scheme for the operation of ST based meshed hybrid distribution network with optimal active/reactive powers control of DG converters.
- 2) To propose the method of determining power flow solution in ST based meshed hybrid distribution network.
- 3) To propose the optimal control method for DG converters in meshed hybrid distribution network.
- 4) To compare the proposed method with the existing literature considering the performance indicators such as operating energy costs, energy loss, voltage profile and sizing of ST converters.

The organization of the paper is as follows. Section II describes the considered system. Section III and Section IV discuss the proposed power management scheme and method of determining power flow solution for ST based meshed hybrid distribution network. Section V explains the DG converters control methodology which includes proposed optimal control of DG converters. The obtained results are given in Section VI. The performance comparison of proposed method with the existing work and conclusions are presented in Section VII and Section VIII, respectively.

II. SYSTEM DESCRIPTION

A CIGRE LV residential distribution network connected to medium voltage ac (MVAC) grid through ST is shown in Fig. 1. Fig. 1(a) shows ST based distribution network without dc line [26], [27]. Fig. 1(b) shows ST based meshed hybrid distribution network with dc line [24]. The dc line is connected through an isolated dc-dc converter to isolate ac and dc networks. This converter is used to improve quality and reliability of power during faulty conditions towards ac and dc buses of the system. The per meter resistance values of the dc line are considered the same as that of resistance of ac line [24]. The MVAC grid is connected to LVAC grid through an ST. The various components present in the system are described as follows.

A. SMART TRANSFORMER

A three stage ST consisting of three power electronics converters are considered in this paper. These converters are an ac-dc converter called as MV converter, the isolated dc-dc converter and dc-ac converter known as LV converter. The ST MV converter is used to maintain the MV dc (MVDC) voltage at a fixed value, and at the same time draws currents from MVAC grid side at unity power factor. These currents are used to support the loads at LVAC side. The isolated dc-dc converter maintains ST LVDC link voltage at a constant value. It also controls the power flow balance between LVDC and MVDC links. The ST LV converter is used to maintain a three-phase balanced sinusoidal voltage at the ST LVAC terminal. The LVDC link of ST is used to form an LVDC line. For better safety and reliability, an additional dc-dc isolated converter is used to interface the LVDC line and ST LVDC bus.

B. LOADS AND DG SOURCES

Residential loads from L1 to L5 connected at various load buses such as 7 to 11 respectively. Along with the loads DG sources such as PV and wind power sources are connected to the dc line through dc/dc converters and ac/dc converters respectively. The PV sources i.e., PV 1, PV 2 and PV 3 are connected at dc buses 13, 15 and 16 respectively. There is one wind power source connected at dc bus 16. The DG sources are considered to be operating at maximum power point (MPP).

C. DG CONVERTERS

The DG sources are connected to ac load bus through dc/ac converters which are known as DG converters. The rated parameters of loads and DG converters connected at various buses are given in Table 1. With this configuration, when sufficient DG power is not present to balance the load requirement, the DG converters can draw power from MVAC grid through the LVDC line. Similarly, when excess power is available with DG sources it can be injected to MVAC grid through LVDC line. This power flow through the dc line improve load voltage profile due to less voltage drop across the dc line. This is possible due to the operation of dc line

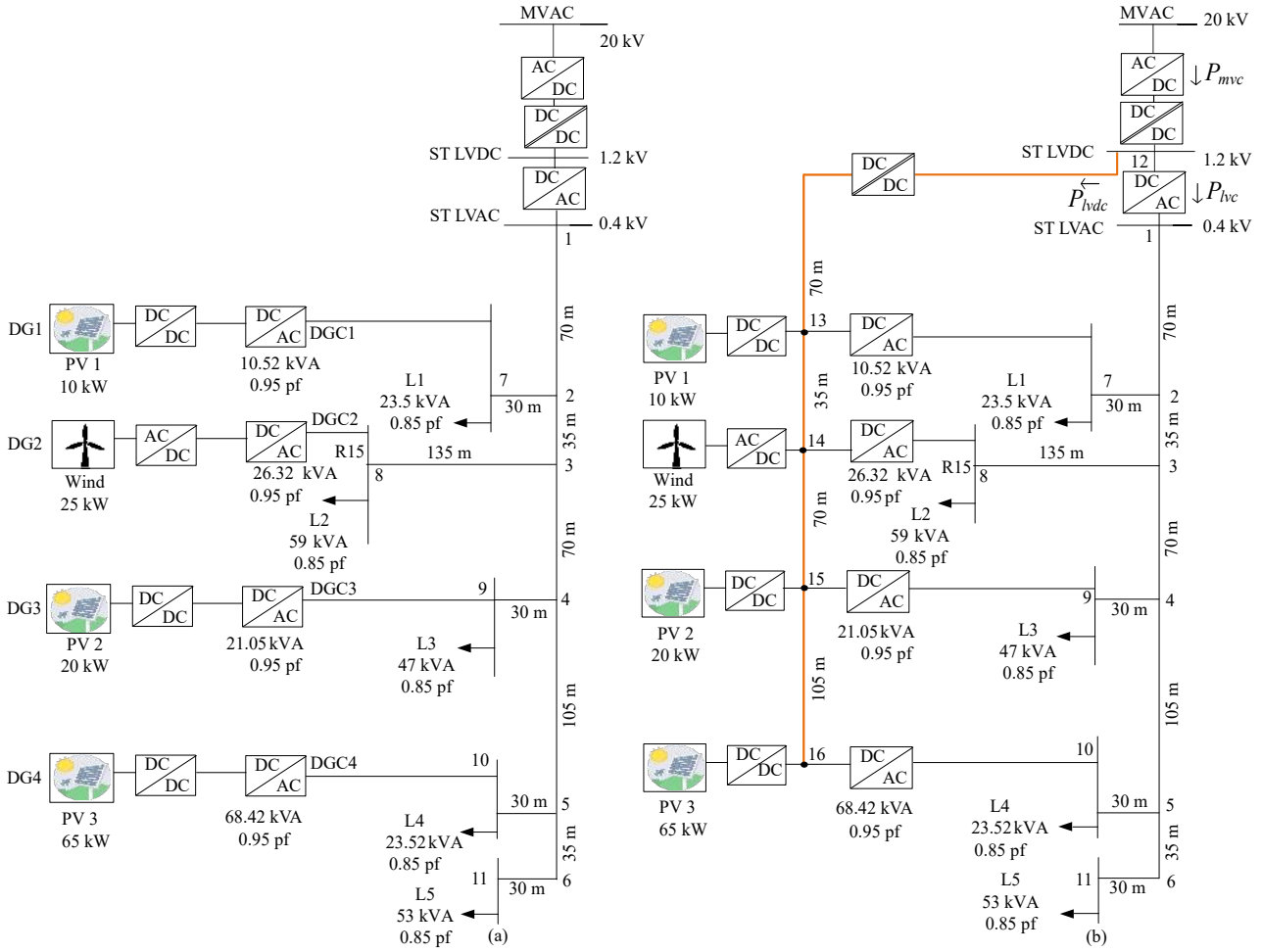


FIGURE 1. (a) Traditional CIGRE LV residential distribution network connected to MVAC grid through ST [26], [27]. (b) Meshed hybrid CIGRE LV residential distribution network connected to MVAC grid through ST.

at high voltage. At the same time, the DG converters do not control their DC link voltage as it is taken care by ST.

III. PROPOSED POWER MANAGEMENT SCHEME

Power management scheme for the system without LVDC line is presented in [25]. The power management scheme in the ST based meshed hybrid distribution network considering the operation of ST converters and DG converters is discussed as follows.

A. OPERATION OF ST CONVERTERS

The operation of ST LV and MV converters is discussed as follows:

1) Operation of ST LV Converter

Considering that the DG converters supply active and reactive powers (P_{dgc} and Q_{dgc} respectively), the ST LV converters supply remaining power to satisfy total load power and ac line loss. In this scenario, active and reactive powers supplied by ST LV converter (P_{lvc} and Q_{lvc} respectively) are given as

follows.

$$P_{lvc}(t) = \sum_{i=1}^{n_l} P_l^i(t) + P_{ac-loss}(t) - \sum_{j=1}^{n_{dg}} P_{dgc}^j(t). \quad (1)$$

$$Q_{lvc}(t) = \sum_{i=1}^{n_l} Q_l^i(t) + Q_{ac-loss}(t) - \sum_{j=1}^{n_{dg}} Q_{dgc}^j(t) \quad (2)$$

where the time 't' represents the time interval $[(t-1) \times T_c, t \times T_c]$, T_c is the control horizon which is equal to one hour, i and j are load and DG source indices, n_l and n_{dg} are the number of loads and DG sources, P_l^i and Q_l^i are the active and reactive powers of i^{th} load, $P_{ac-loss}$ and $Q_{ac-loss}$ are the active and reactive power losses in ac line. Considering that the DG sources supply active power (P_{dg}), the ST LVDC grid supplies remaining power to satisfy total DG converters active power and dc line loss. In this scenario, the active power drawn from LVDC grid (P_{lvdc}) is given as follows:

$$P_{lvdc}(t) = \sum_{j=1}^{n_{dg}} P_{dgc}^j(t) - \sum_{j=1}^{n_{dg}} P_{dg}^j(t) + P_{dc-loss}(t) \quad (3)$$

TABLE 1. Rated Parameters of Loads and DG converters

Component	Apparent Power (kVA)	pf
L1	23.5	0.85
L2	59	0.85
L3	47	0.85
L4	23.52	0.85
L5	53	0.85
DGC1	10.52	0.95
DGC2	26.32	0.95
DGC3	21.05	0.95
DGC4	68.42	0.95

where $P_{dc-loss}$ is the dc line loss. The total power loss is the sum of the ac and dc line losses in the system.

2) Operation of ST MV Converter

The active power supplied by the MV converter (P_{mvc}) is the sum of the active powers supplied by ST at its LVAC and LVDC terminals. The MV converter of ST is not used to supply reactive power. Therefore P_{mvc} and reactive power supplied by ST MV converter (Q_{mvc}) are given as follows.

$$P_{mvc}(t) = P_{lvac}(t) + P_{lvdc}(t). \quad (4)$$

$$Q_{mvc}(t) = 0. \quad (5)$$

B. OPERATION OF DG CONVERTERS

The DG converters operation when they are supplying only active power is discussed in [24]. According to that active power reference ($P_{dgc-ref}^j$) is generated in proportion to DG converters kVA rating i.e.,

$$P_{dgc-ref}^j(t) = \frac{P_{tl}(t) \times S_{dgc-r}^j}{\sum_{j=1}^{n_{dg}} S_{dgc-r}^j}, \quad P_{tl}(t) < \sum_{j=1}^{n_{dg}} S_{dgc-r}^j \quad (6)$$

$$= S_{dgc-r}^j, \quad \text{otherwise}$$

where P_{tl} is the total load active power requirement and S_{dgc-r}^j is the kVA rating of j^{th} DG converter. However, this method of obtaining DG converters powers is not optimal method.

In the proposed method DG converters are used to supply both active and reactive powers. The DG converters provide active and reactive powers as per the given $P_{dgc-ref}^j$ and reactive power references ($Q_{dgc-ref}^j$).

$$P_{dgc}^j(t) = P_{dgc-ref}^j(t). \quad (7)$$

$$Q_{dgc}^j(t) = Q_{dgc-ref}^j(t). \quad (8)$$

The $P_{dgc-ref}^j$ and $Q_{dgc-ref}^j$ are generated through the proposed optimal DG converters control method.

IV. PROPOSED POWER FLOW SOLUTION METHOD

The determination of optimal DG converters references requires power flow solution. This section explains the proposed method of determining power flow solution in ST

TABLE 2. Type of buses in ST meshed hybrid distribution network

Type	Slack bus	Load bus
LVAC network	1	2-11
LVDC network	12	13-16

based meshed hybrid distribution network. The ST based network without dc line is a 11-bus system as shown in Fig. 1(a). For this the power flow solution is obtained considering ST LVAC terminal i.e., bus 1 as slack bus and remaining buses are considered as load buses [28]. The ST based meshed hybrid distribution network is a 16-bus system as shown in Fig. 1(b). For obtaining power flow solution, it is important to know the type of buses and bus data.

A. TYPE OF BUSES

In the considered system there are both ST LVAC and LVDC terminals connected to loads. In this scenario, the whole network is divided into two networks as LVAC network and LVDC network. The LVAC network consists of buses 1-11 and LVDC network consists of buses 12-16. Here the ST LVAC and LVDC bus voltages are maintained at 1 p.u. Therefore, the power flow equations are solved independently for LVAC and LVDC networks considering ST LVAC and LVDC buses (bus 1 and bus 12) as slack buses. All the remaining buses are considered as load buses. The types of buses in these networks are shown in Table 2.

B. BUS DATA

Note that the DG converters powers are common while solving the power flow solution of the LVAC and LVDC networks. The load bus power at each load bus in LVAC network (P_{lbac}) is given in (9).

$$P_{lbac}(t) = P_l(t) - P_{dgc}(t). \quad (9)$$

The load bus power at each load bus in LVDC network (P_{lbdc}) is given in (10).

$$P_{lbdc}(t) = P_{dgc}(t) - P_{dg}(t). \quad (10)$$

Using load bus powers as bus data, backward forward sweep power flow method is applied to both LVAC and LVDC networks in order to obtain required power flow solution in the system [29].

V. PROPOSED OPTIMAL CONTROL METHOD OF DG CONVERTERS

An optimal control method to generate optimal active and reactive power references of DG converters ($P_{odgc-ref}^j$ and $Q_{odgc-ref}^j$) is proposed. The overview of proposed optimal control method of DG converters is shown in Fig. 2. The figure shows that the proposed control method provides optimal DG converters active and reactive power references as output considering load powers and DG source powers as input. The formulation of optimization problem is discussed as follows.

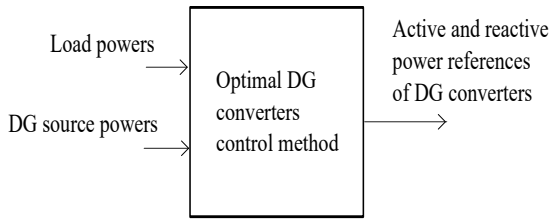


FIGURE 2. Overview of proposed DG converters control method.

A. OPTIMIZATION PROBLEM FORMULATION

The optimization problem is formulated for determining $P_{odgc-ref}^j$ and $Q_{odgc-ref}^j$ for DG converters. The operating energy costs of the system mainly depends on the energy drawn from STMV grid. Therefore, minimization of energy drawn from STMV grid is considered as the objective. Moreover, there are several constraints to be satisfied for normal operation of the system. Firstly, the power balance constraint i.e., the active power drawn from MVAC grid is the sum of active powers drawn from ST LVAC and LVDC terminals. Also, the load bus voltages should be maintained within the limits specified by the grid code. Along with these constraints the kVA supplied by the DG converters should be less than its kVA rating and the power factor of DG converter should be maintained above certain minimum limit. These fitness function and constraints are given from (11)-(15), respectively,

$$\text{minimize } f = E_{mvac}(t) + dp. \quad (11)$$

subjected to

- 1) Power balance constraint

$$P_{mvac}(t) = P_{lvc}(t) + P_{lvdc}(t). \quad (12)$$

- 2) Load bus voltage constraint

$$V_{min} \leq V_l^i(t) \leq V_{max}. \quad (13)$$

- 3) DG converters rating constraint

$$\sqrt{(P_{dgc-ref}^j(t))^2 + (Q_{dgc-ref}^j(t))^2} \leq S_{dgc-r}^j. \quad (14)$$

- 4) DG converters power factor constraint

$$pf_{dgc-min} \leq pf_{dgc}^j(t) \leq 1. \quad (15)$$

where P_{mvac} is the active power drawn from MVAC grid, dp is the death penalty, V_{min} and V_{max} are the minimum and maximum bus voltage magnitude limits given by grid code. These are chosen as 0.95 p.u. and 1.05 p.u., respectively [30], V_l^i is the magnitude of voltage at i^{th} load, pf_{dgc}^j is the power factor of j^{th} DG converter and $pf_{dgc-min}$ is the minimum power factor to be maintained for DG converters which is chosen as 0.8 [22], [31].

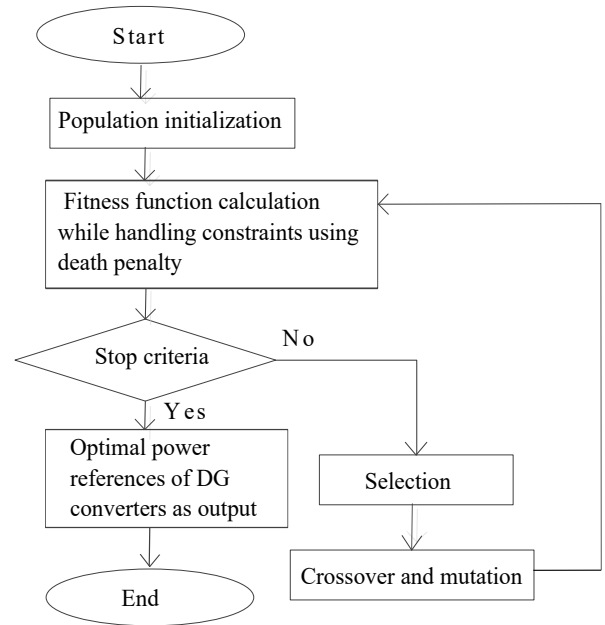


FIGURE 3. Determination of optimal powers of DG converters using GA.

B. SOLVING OPTIMIZATION PROBLEM

Equation (11) shows that the objective is to minimize energy drawn from ST MVAC grid (E_{mvac}). The E_{mvac} is given in (16) and calculated using proposed power flow solution method.

$$E_{mvac}(t) = (P_{lvc}(t) + P_{lvdc}(t)) \times T_c. \quad (16)$$

Substituting (1), (3) in (4) gives,

$$E_{mvac}(t) = \left(\sum_{i=1}^{n_l} P_l^i(t) + P_{ac-loss}(t) - \sum_{j=1}^{n_{dg}} P_{dg}^j(t) + P_{dc-loss}(t) \right) \times T_c. \quad (17)$$

The constraints are handled using death penalty method. This method is a simple way of handling constraints [32]. According to this the unfeasible solutions from the population are discarded if any of the constraint is violated. The death penalty is applied considering that all the constraints i.e., bus voltage magnitudes, DG converters ratings should be strictly satisfied without any violations. Accordingly $dp = 0$, if there are no constraint violations and $dp = inf$, if there is any constraint violation [33].

The considered fitness function is a nonlinear function. Therefore, the proposed optimal control problem is solved using GA with ga solver in MATLAB. Because GA is a popular method for solving optimization problems with nonlinear fitness function [34]. In GA it is important to chose parameters such as population size, rate of mutation and crossover etc., carefully to avoid the possible risk of non-convergence. If they are chosen inappropriately it will be difficult for the algorithm to converge or it will produce meaningless results [34]. The default values are chosen for various parameters of

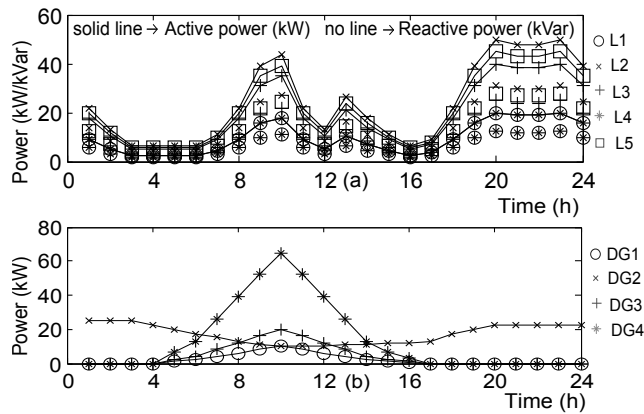


FIGURE 4. (a) Loads power profiles [35]. (b) DG sources power profiles [36].

GA, except for population size. The population size is tuned such that three different runs converges precisely to the same value. It is chosen as 80.

The method of solving optimization problem using GA is shown as a flowchart in Fig. 3. According to that firstly population initialization is done. Then fitness function is calculated using (17). This calculation of fitness function is repeated through selection, crossover and mutation till the stop criteria is reached. The GA uses certain options to determine when to stop. Some of those options are maximum number of generations (iterations) and function tolerance i.e., it runs until the average relative change in the fitness function value is less than given function tolerance if any etc. If any one of these options is satisfied, the GA stops doing iterations and provides results. In this work, the maximum number of iterations are not specified for GA. They are chosen by default. The default maximum number of iterations are 100 times the number of control variables. Once the stop criteria is reached the algorithm provides optimal active and reactive power references of DG converters as output.

VI. SIMULATION RESULTS

The proposed method is tested in MATLAB since the optimal power flow analysis is required as per the proposed method. In this study the performance of proposed control method is tested for load demand and DG source power profiles over a day. While doing the optimization using GA method, these values are called and used for providing optimal active and reactive power references for DG converters at each time t . The hourly load power profiles over a day are shown in Fig. 4(a), where peak load occurs during 20:00 and 23:00 hours [35]. The hourly DG power profiles over a day are shown in Fig. 4(b) [36]. The obtained results for these power profiles are discussed as follows.

A. CASE 1: ST WITHOUT DC LINE

1) DG Converters Powers

In this case the DG converters are considered to be operating at unity power factor. Therefore they are not used to provide

reactive power. The active power supplied by DG converters depends on the available DG sources power which are operating at maximum power point. These active powers supplied by DG converters are shown in Fig. 5(a). The DG converters 1,3 and 4 provide active powers as per the availability of PV generation of PV 1,2 and 3 respectively. The DG converter 2 provides active power as per the availability of wind source power. For example at $t = 1$ h, the DG converter 1, 2, 3 and 4 powers are 0, 25, 0, 0 kW respectively.

2) Load Bus Voltages and Power Loss

The load bus voltage profile and power loss are obtained using the power flow solution method. The resulting voltage profile is shown in Fig. 5(b). It that there are no voltage rise violations in the network. However, there are voltage drop violations in the network during peak load hours. For example the load bus voltage at L5 is less than 0.95 p.u. at $t = 20$ h. The resulting power loss profile is shown in Fig. 5(c). It is observed that the power loss is maximum during peak load hours. The power loss at peak load hour of $t = 20$ h is 13.155 kW.

3) ST Converters Powers

The active, reactive and apparent powers supplied by ST LV converter are shown in Fig. 5(d). Since the DG converters do not supply any reactive power, the entire load reactive power is supplied by ST LV converter. The peak ST LV active power is 165.655 kW at $t = 20$ h. The ST MV converter does not supply any reactive power as it is operated at unity power factor. The active power supplied by ST MV converter is shown in Fig. 5(e). It is same as that of active power supplied by ST LV converter.

B. CASE 2: ST BASED MESHED HYBRID SYSTEM WHERE DG CONVERTERS OPERATE AT UNITY POWER FACTOR [24]

1) DG Converters Powers

In this case the DG converters are considered to be operating at unity power factor. Therefore they are not used to provide reactive power. The DG converters supply active power in proportion to their ratings as given in (6). These active powers of DG converters are shown in Fig. 6(a). It is observed that there is active power supplied by the DG converters even when there is no power available from DG sources. This is possible due to the presence of dc line. For example at $t = 1$ h, there is no power available from PV source. However, the DG converter 1 supply active power of 6.3408 kW. Similarly, the DG converter 2, 3 and 4 powers at $t = 1$ h are 15.8521, 12.6817 and 41.2154 kW respectively. It is also observed that when the total load active power is more than the sum of the kVA ratings of DG converters, the DG converters powers are maintained at their respective ratings. For example at peak load hour of $t = 20$ h, the DG converter 1, 2, 3 and 4 powers are 10.52, 26.32, 21.05 and 68.42 kW respectively.

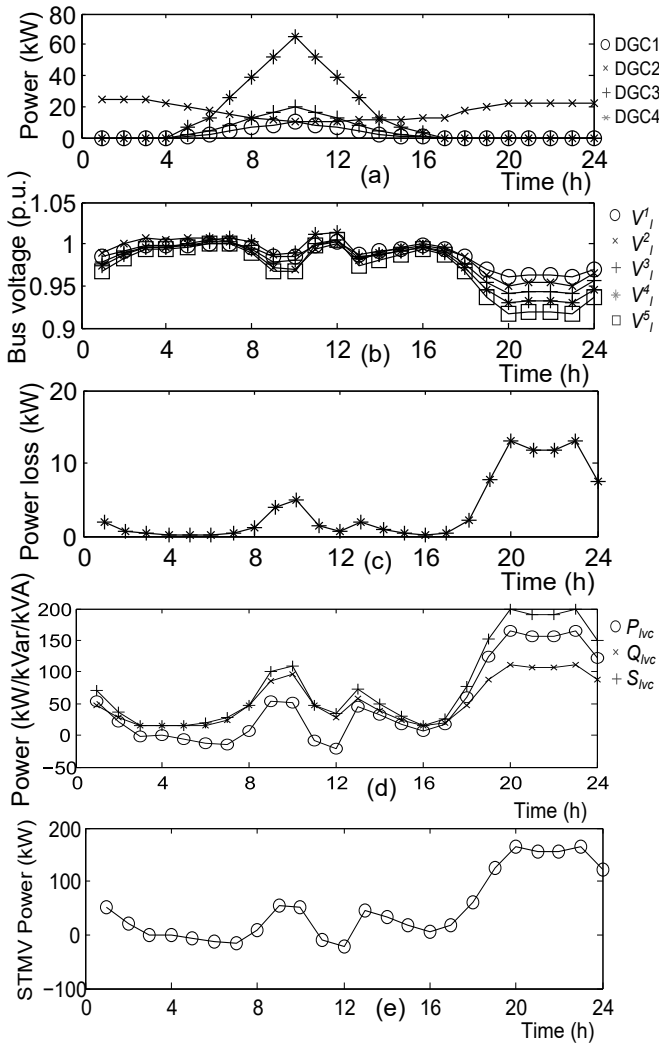


FIGURE 5. Case 1. (a) Power of DG converters. (b) Voltage profile of loads. (c) Power loss. (d) ST LV converters power. (e) ST MV converters power.

2) Load Bus Voltages and Power Loss

The load bus voltage profile and power loss are obtained using the power flow solution method. The voltage profile is shown in Fig. 6(b). It indicates that there are no voltage rise violations in the network. Moreover, there are no voltage drop violations in the network even during peak load hours. It means all the load bus voltages are within 0.95 p.u. at all the times of the day. The obtained power loss profile is shown in Fig. 6(c). It indicates that the power loss at all the times of the day is less than the power loss of Case 1. For example at peak load hour of $t = 20$ h, the power loss is 6.8350kW which is less than that of Case 1. This is due to presence of dc line which allows the power flow through it.

3) DG Converters Powers

The active, reactive and apparent powers supplied by ST LV converter are shown in Fig. 6(d). Since the DG converters do not supply any reactive power, the entire load reactive power is supplied by ST LV converter. The ST LV active and re-

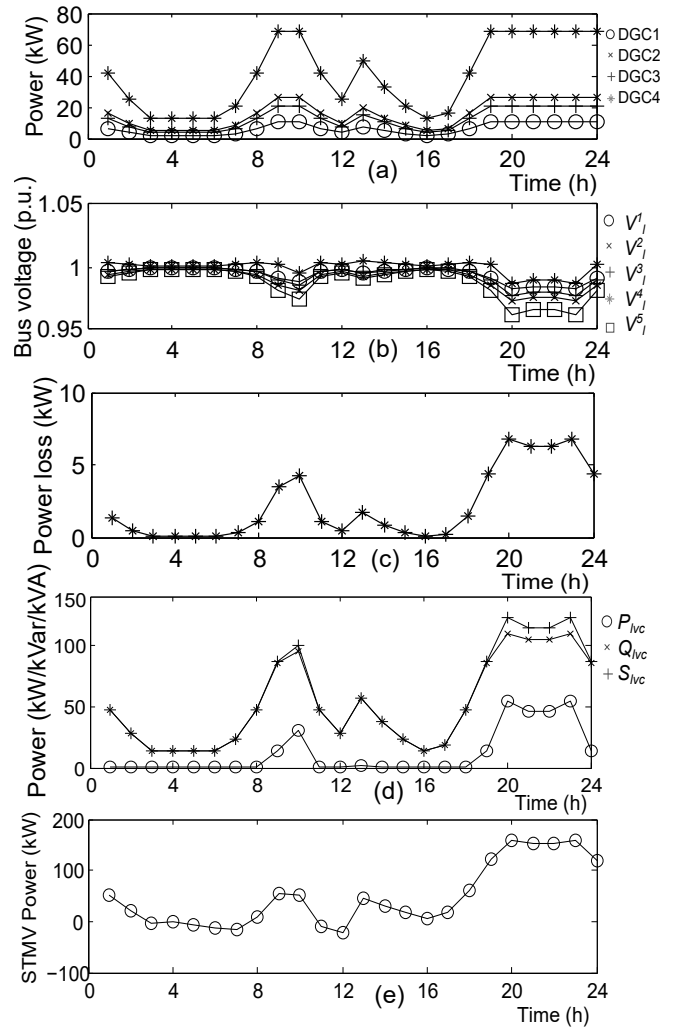


FIGURE 6. Case 2. (a) Power of DG converters. (b) Voltage profile of loads. (c) Power loss. (d) ST LV converters power. (e) ST MV converters power.

active powers are determined using (1) and (2), respectively. The peak ST LV active power is 54.5795 kW at $t = 20$ h. The ST MV converter does not supply any reactive power as it is operated at unity power factor. The active power supplied by ST MV converter determined using (4) and shown in Fig. 6(e). The peak ST MV power is 159.335 kW at $t = 20$ h.

C. CASE 3: ST BASED MESHED HYBRID SYSTEM WHERE DG CONVERTERS OPERATE USING PROPOSED METHOD

1) DG Converters Powers

In this case, the optimal active and reactive powers of DG converters are determined using Fig. 3. In GA, it is possible that different runs provide different optimal results for the chosen parameters. Therefore, in this paper GA is run multiple times at $t=1$, to check the results of optimization for the considered population size. The plot of best fitness values for multiple runs of genetic algorithm is shown in Fig. 7. It is observed that all the runs provided same optimal result i.e., the minimum of best fitness values is same in all

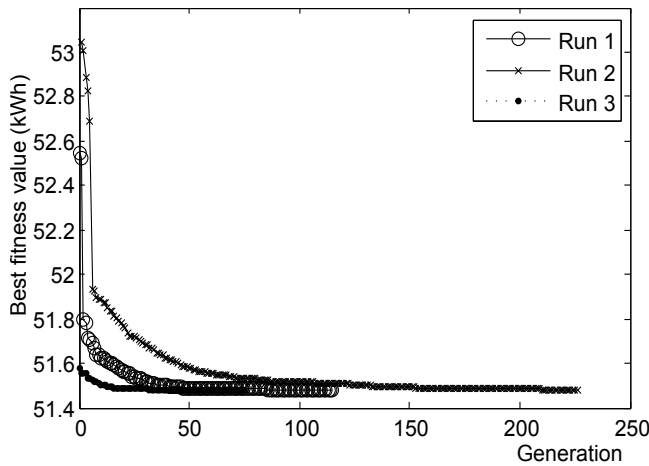


FIGURE 7. Best fitness values for multiple runs at $t = 1$.

the runs which is equal to 51.42 kWh. It means the optimal energy drawn from the ST MVAC grid at $t=1$ h is 51.42 kWh. Similarly, optimal energy values drawn from the ST MVAC grid over a day are obtained. The corresponding optimal active and reactive powers of DG converters are shown in Fig. 8(a). The DG converter 1, 2, 3 and 4 active powers at $t = 1$ h are 9.0999, 22.6424, 16.1172 and 19.0303 kW respectively. Similarly, the DG converter 1, 2, 3 and 4 reactive powers at $t = 1$ h are 5.2743, 13.4064, 12.0761, 13.9951 kVar respectively.

2) Load Bus Voltages and Power Loss

The load bus voltage profile and power loss are obtained using the power flow solution method. The resulting voltage profile is shown in Fig. 8(b). It indicates that there are no voltage rise violations in the network. Moreover, there are no voltage drop violations in the network even during peak load hours. It means all the load bus voltages are within 0.95 p.u. at all the times of the day. The power loss profile over a day is shown in Fig. 8(c). It indicates that the power loss at all the times of the day is less than the power loss of Case 1. For example at peak load hour of $t = 20$ h, the power loss is 4.1381 kW which is less than that of Case 1 and 2. This is due to the application of proposed optimal control of DG converters control in the system.

3) ST Converters Powers

The active, reactive and apparent powers supplied by ST LV converter are shown in Fig. 8(d). Since the DG converters do not supply any reactive power, the entire load reactive power is supplied by ST LV converter. The ST LV active and reactive powers are determined using (1) and (2), respectively. The peak ST LV active power is 67.5446 kW at $t = 20$ h. The ST MV converter does not supply any reactive power as it is operated at unity power factor. The active power supplied by ST MV converter determined using (4) and shown in Fig. 8(e). The peak ST MV power is 156.6381 kW at $t = 20$ h.

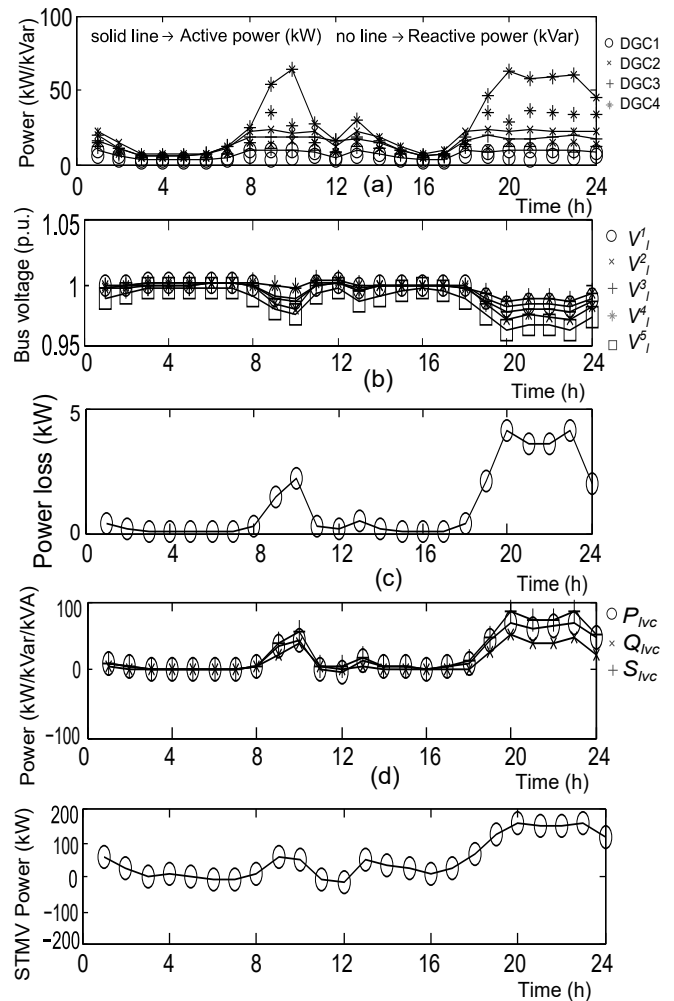


FIGURE 8. Case 1. (a) Optimal active/reactive powers of DG converters. (b) Voltage profile of loads. (c) Power loss. (d) ST LV converters power. (e) ST MV converters power.

In this case both active/reactive powers of DG converters are controlled using proposed method. Since the reactive power is supplied locally using DG converters located at load terminals, the reactive power requirement of the STLV converter is reduced. Further, the DG converters active/reactive powers are optimally controlled to minimize the energy drawn from MVAC grid while satisfying the load bus voltage constraints. These are the main advantages of proposed method.

Further, the performance comparison of the proposed method i.e., Case 3 with other two cases and possibility of real time application of proposed work is discussed in following section.

VII. PERFORMANCE COMPARISON AND POSSIBILITY OF REAL-TIME APPLICATION OF PROPOSED WORK

The performance of the three cases is compared considering the performance indicators such as operating energy cost, energy loss, voltage profile and sizing of ST converters.

TABLE 3. Time-of-use price [37]

Time	Energy price (INR/kWh)
Peak time	5.39
Off-peak time	4.15
Remaining time	4.39

A. PERFORMANCE COMPARISON

1) Energy Loss

Energy loss over a day (EL) is calculated using (18),

$$EL = \sum_{t=1}^T P_{loss}(t) \times T_c. \quad (18)$$

The EL for Case 1, Case 2, and Case 3 are 86.3205, 52.126, and 25.5420 kWh/day, respectively. It means that there is a percentage of 39.61% energy loss reduction with Case 2 (ST based meshed hybrid distribution network and control of DG converters at unity power factor) as compared to Case 1 (ST without dc line and DG converters are operated as per DG sources power availability). This is because the power flow in the dc line leads to less power loss as the dc line is operated at higher voltage.

Moreover, there is a percentage of 70.41% energy loss reduction with Case 3 (ST based meshed distribution network and DG converters controlled using proposed method) as compared to Case 1. It means that the energy loss is reduced by 30.8% with Case 3 as compared to Case 2. This is because in Case 3, both active/reactive powers of DG converters are controlled optimally using proposed method. Therefore, the power loss in the system is further reduced as compared to Case 2.

2) Operating Energy Costs

The operating energy costs of the system over the day (OC) are calculated using (19),

$$OC = \sum_{t=1}^T E_{grid-d}(t) \times EP(t) \quad (19)$$

where T is the operating horizon of 24 hours, i.e., $T = 24$ hours, E_{grid-d} is the energy demand of the ST MVAC grid and EP is the energy price of the system. The E_{grid-d} is determined as given in (20),

$$E_{grid-d}(t) = E_{mvac}(t), \text{ if } E_{mvac}(t) \geq 0 \\ = 0, \text{ otherwise.} \quad (20)$$

For this, the time-of-use price of the energy is considered [38]. It is considered that when load demand is more than 75% of the peak load, it is peak time. When load demand is less than 25% of the peak load, it is off-peak time. The EP values are given in Table 3 [37]. For this, the OC for Case 1, Case 2, and Case 3 are determined as 6508.5, 6331.2, and 6201.7 INR/day, respectively. It means that there is a percentage of 2.72% operating energy cost reduction with Case 2 as compared to Case 1. This is due to the reduction

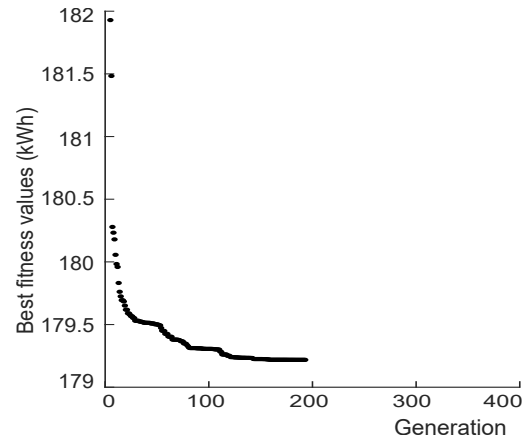


FIGURE 9. Best fitness values for various generations in worst case scenario.

of the power loss in the system with Case 2 as compared to Case 1.

Moreover, there is a percentage of 4.71% operating energy cost reduction with Case 3 as compared to Case 1. It means that the operating energy cost is reduced by 1.99% with Case 3 as compared to Case 2. This is due to the reduction of the power loss in the system with proposed control of DG converters as compared to Case 2.

3) Voltage Profile

The average voltage deviation index (V_{ad}) is considered along with the worst maximum and minimum bus voltages (V_{wmin} and V_{wmax}) [28] to know the voltage profile of the system. The V_{ad} is determined using (21)

$$V_{ad} = \frac{\sum_{t=1}^T \sum_{i=1}^{n_l} (V_l^i(t) - V_{ref})}{T \times n_l} \quad (21)$$

where V_{ref} is the reference voltage of 1 p.u. The value of V_{ad} should be low for better system voltage profile (bus voltages are close to 1 p.u.).

The V_{wmin} for Case 1, Case 2 and Case 3 are 0.9156, 0.9623 and 0.9636 p.u., respectively. This shows that there are voltage drop violations for Case 1. However, there are no voltage drop violations with Case 2 and Case 3. Moreover, V_{wmin} is more for Case 3 as compared to Case 1 and Case 2. The V_{wmax} for Case 1, Case 2 and Case 3 are 1.0135, 1.0048 and 1.0023 p.u., respectively which indicates that there are no voltage rise violations for three cases. However, V_{wmax} is less for Case 3 as compared to Case 1 and Case 2. The V_{ad} for Case 1, Case 2 and Case 3 are 0.0212, 0.0078, 0.0074 p.u., respectively. The V_{ad} for Case 2 is reduced by a percentage of 63.21% as compared to Case 1. The V_{ad} for Case 3 is reduced by a percentage of 65.09% as compared to Case 1.

This indicates that the voltage profile in Case 2 and Case 3 is significantly improved as compared Case 1. This is because the power flow through the dc line causes less voltage drop across the dc line as it is operating at a higher voltage. The voltage profile is not significantly improved in Case 3 as compared to Case 2. Because in Case 3 the DG converters are

optimally controlled for minimizing the MVAC grid energy while satisfying the load bus voltage constraints.

4) Sizing of ST Converters

To show the impact of optimal DG converters control on sizing of ST converters a worst case scenario is considered. The worst case scenario is when the load demand is at its peak and there is no DG sources power available. In this scenario, load demands of L1, L2, L3, L4 and L5 are 20, 50, 40, 20, 45 kW, respectively. Power from PV sources and wind source is 0 kW. The required kVA rating of LV converter (S_{lvc-r}) is determined using ST LV converters active and reactive powers in this worst case scenario ($P_{lvc-wcs}$ and $Q_{lvc-wcs}$, respectively) as given in (22),

$$S_{lvc-r} = \sqrt{(P_{lvc-wcs})^2 + (Q_{lvc-wcs})^2}. \quad (22)$$

Similarly, the required kVA rating of MV converter (S_{mvc-r}) is determined using peak ST MVAC active and reactive powers ($P_{mvc-wcs}$ and $Q_{mvc-wcs}$, respectively) as given in (23)

$$S_{mvc-r} = \sqrt{(P_{mvc-wcs})^2 + (Q_{mvc-wcs})^2}. \quad (23)$$

Case 1

In this case, the S_{lvc-r} is calculated as 221.3655 kVA using (22). Similarly, the S_{mvc-r} is calculated as 190.6915 kVA using (23).

Case 2

For this case, the P_{lvc} and Q_{lvc} are determined using (1) and (2), respectively. Then using (22), the S_{lvc-r} is calculated as 122.5742 kVA. It means that the size of ST LV converter for Case 2 is reduced by a percentage of 44.63% as compared to Case 1. This is because, even when there is no DG sources power the DG converters are used to supply power using (6). This power is drawn from the LVDC line. With this the power requirement from ST LV converter is reduced which led to the reduction of its size.

Similarly the $P_{mvc-wcs}$ and $Q_{mvc-wcs}$ are determined using (4) and (5), respectively. Then using (23), the S_{mvc-r} is calculated as 181.9410 kVA. It means that the size of ST MV converter for Case 2 is reduced by a percentage of 4.59% as compared to Case 1. This is due to the reduction of power loss in Case 3 as compared to Case 2.

Case 3

In this case, the best fitness values for various generations for worst case scenario are shown in Fig. 9. The P_{lvc} and Q_{lvc} are determined using (1) and (2), respectively. Then using (22), the S_{lvc-r} is calculated as 84.3321 kVA. It means that the size of ST LV converter for Case 3 is reduced by a percentage of 61.9% as compared to Case 1. This indicates the size of ST LV converter for Case 3 is reduced by a percentage of 17.27% as compared to Case 2. This is because in Case 3, DG converters are used to supply the reactive

power optimally along with the active power. Therefore, the reactive power requirement of ST LV converter is reduced which led to the reduction of its size.

Similarly the $P_{mvc-wcs}$ and $Q_{mvc-wcs}$ are determined using (4) and (5), respectively. Then using (23), the S_{mvc-r} is calculated as 179.2184 kVA. It means that the size of ST MV converter for Case 3 is reduced by a percentage of 6.02% as compared to Case 1. This indicates the size of ST MV converter for Case 3 is reduced by a percentage of 1.43% as compared to Case 2. This is due to the reduction of power loss in Case 3 as compared to Case 2.

The quantitative comparison of three cases considering the above performance indicators is given in Table 4. It shows the significant improvement in the performance indicators with the optimal control of DG converters. Note that the performance mainly depends on available DG sources powers over the day and DG converters ratings. If the DG converters ratings are increased, the cost savings will be improved and size of ST converters will be reduced further.

B. POSSIBILITY OF REAL-TIME APPLICATION OF PROPOSED WORK

It is possible to implement the proposed method in larger grids depending the available DG converters and their control capabilities. However, the real-time application of proposed work mainly requires measurement devices to measure load and DG powers. Further, it requires communication infrastructure for data transfer to the controller. Because in order to determine the optimal active/reactive powers of DG converters it requires load power and DG power as input.

There are certain challenges like communication delay, secure data transmission. However, there is extensive work presented in literature to avoid these challenges. For example, the useful methods to avoid the issues such as delays and secure data transmission are proposed in [39] and [40] respectively. With these available literature, it is possible to realize the proposed control method in real time.

VIII. CONCLUSIONS

This paper presents the impact of optimal control of DG converters in ST based meshed hybrid distribution network. The obtained results show that the energy loss and operating energy costs are reduced by 30.8% and 1.99%, respectively over a day using the proposed method as compared to the case when DG converters supply only active power as per Case 2. Moreover, better system voltage profile is obtained with proposed method as compared to other methods. The ST LV converter and MV converter sizes are reduced by 17.27% and 1.43%, respectively using the proposed method as compared to the case when DG converters supply only active power as per Case 2.

REFERENCES

- [1] T. Ackermann, G. Andersson, and L. Söder, "Distributed generation: a definition," *Electr. Power Syst. Res.*, vol. 57, DOI [https://doi.org/10.1016/S0378-7796\(01\)00101-8](https://doi.org/10.1016/S0378-7796(01)00101-8), no. 3, pp. 195 – 204, 2001.

TABLE 4. Quantitative Comparison of Three Cases

Type	OC (INR/day)	EL (kWh/day)	V_{wmin} (p.u.)	V_{wmax} (p.u.)	V_{ad} (p.u.)	S_{lvc-r} (kVA)	S_{mvc-r} (kVA)
Case 1	6508.5	86.3205	0.9156	1.0135	0.0212	221.3655	190.6915
Case 2 [24]	6331.2	52.126	0.9623	1.0048	0.0078	122.5742	181.9410
Case 3	6201.7	25.5420	0.9636	1.0023	0.0074	84.3321	179.2184

[2] S. Lakshmi and S. Ganguly, "Simultaneous optimisation of photovoltaic hosting capacity and energy loss of radial distribution networks with open unified power quality conditioner allocation," *IET Renew. Power Gener.*, vol. 12, no. 12, pp. 1382–1389, 2018.

[3] S. Lakshmi and S. Ganguly, "An on-line operational optimization approach for open unified power quality conditioner for energy loss minimization of distribution networks," *IEEE Trans. Pow. Sys.*, vol. 34, no. 6, pp. 4784–4795, 2019.

[4] A. A. Abou El-Ela, R. A. El-Sehiemy, A. Kinawy, and M. T. Mouwafi, "Optimal capacitor placement in distribution systems for power loss reduction and voltage profile improvement," *IET Gener. Transm. Distrib.*, vol. 10, no. 5, pp. 1209–1221, 2016.

[5] S. Ganguly and D. Samajpati, "Distributed generation allocation on radial distribution networks under uncertainties of load and generation using genetic algorithm," *IEEE Trans. Sust. Energy*, vol. 6, no. 3, pp. 688–697, 2015.

[6] R. Pegado, Z. Naupari, Y. Molina, and C. Castillo, "Radial distribution network reconfiguration for power losses reduction based on improved selective bpsos," *Electr. Power Syst. Res.*, vol. 169, DOI <https://doi.org/10.1016/j.epr.2018.12.030>, pp. 206 – 213, 2019.

[7] D. Das, "Optimal placement of capacitors in radial distribution system using a fuzzy-ga method," *Int. J. Elect. Power Energy Syst.*, vol. 30, DOI <https://doi.org/10.1016/j.ijepes.2007.08.004>, no. 6, pp. 361 – 367, 2008.

[8] M. Ahmed, L. Meegahapola, A. Vahidnia, and M. Datta, "Stability and Control Aspects of Microgrid Architectures—A Comprehensive Review," *IEEE Access*, vol. 8, DOI [10.1109/ACCESS.2020.3014977](https://doi.org/10.1109/ACCESS.2020.3014977), pp. 144 730–144 766, 2020.

[9] R. Rosso, X. Wang, M. Liserre, X. Lu, and S. Engelken, "Grid-Forming Converters: Control Approaches, Grid-Synchronization, and Future Trends—A Review," *IEEE Open J. Ind. Appl.*, vol. 2, DOI [10.1109/OJIA.2021.3074028](https://doi.org/10.1109/OJIA.2021.3074028), pp. 93–109, 2021.

[10] V. Sarfi and H. Livani, "Optimal Volt/VAR control in distribution systems with prosumer DERs," *Electr. Power Syst. Res.*, vol. 188, DOI <https://doi.org/10.1016/j.epr.2020.106520>, p. 106520, 2020.

[11] X. Liu, P. Wang, and P. C. Loh, "A hybrid ac/dc microgrid and its coordination control," *IEEE Trans. Smart Grid*, vol. 2, no. 2, pp. 278–286, 2011.

[12] X. Liang, "Emerging power quality challenges due to integration of renewable energy sources," *IEEE Trans. Ind Appl.*, vol. 53, no. 2, pp. 855–866, 2017.

[13] C. Kumar, R. Zhu, G. Buticchi, and M. Liserre, "Sizing and soc management of a smart-transformer-based energy storage system," *IEEE Trans. Ind. Electron.*, vol. 65, no. 8, pp. 6709–6718, 2018.

[14] S. Bhattacharya, "Transforming the transformer," *IEEE Spectr.*, vol. 54, no. 7, pp. 38–43, 2017.

[15] R. Zhu, M. Andresen, M. Langwasser, M. Liserre, J. P. Lopes, C. Moreira, J. Rodrigues, and M. Couto, "Smart transformer/large flexible transformer," *CES Trans. Elect. Machines Syst.*, vol. 4, DOI [10.30941/CES-TEMS.2020.00033](https://doi.org/10.30941/CES-TEMS.2020.00033), no. 4, pp. 264–274, 2020.

[16] M. Liserre, G. Buticchi, M. Andresen, G. De Carne, L. F. Costa, and Z. Zou, "The smart transformer: Impact on the electric grid and technology challenges," *IEEE Ind. Electron. Mag.*, vol. 10, no. 2, pp. 46–58, 2016.

[17] H. V. M., A. K. Deka, and C. Kumar, "Capacity enhancement of a radial distribution grid using smart transformer," *IEEE Access*, vol. 8, pp. 72 411–72 423, 2020.

[18] S. Giacomuzzi, M. Langwasser, G. De Carne, G. Buja, and M. Liserre, "Smart transformer-based medium voltage grid support by means of active power control," *CES Trans. Elect. Machines Syst.*, vol. 4, DOI [10.30941/CES-TEMS.2020.00035](https://doi.org/10.30941/CES-TEMS.2020.00035), no. 4, pp. 285–294, 2020.

[19] A. Gupta, S. Doolla, and K. Chatterjee, "Hybrid ac-dc microgrid: Systematic evaluation of control strategies," *IEEE Trans. Smart Grid*, vol. 9, DOI [10.1109/TSG.2017.2727344](https://doi.org/10.1109/TSG.2017.2727344), no. 4, pp. 3830–3843, 2018.

[20] A. Agrawal, C. S. Nalamati, and R. Gupta, "Hybrid dc-ac zonal microgrid enabled by solid-state transformer and centralized esd integration," *IEEE Trans. Ind. Electron.*, vol. 66, DOI [10.1109/TIE.2019.2899559](https://doi.org/10.1109/TIE.2019.2899559), no. 11, pp. 9097–9107, 2019.

[21] J. Chen, R. Li, A. Soroudi, A. Keane, D. Flynn, and T. O'Donnell, "Smart transformer Modelling in Optimal Power Flow Analysis," in *IECON 2019 - 45th Annual Conference of the IEEE Industrial Electronics Society*, vol. 1, DOI [10.1109/IECON.2019.8926817](https://doi.org/10.1109/IECON.2019.8926817), pp. 6707–6712, 2019.

[22] R. Zhu, M. Liserre, M. Langwasser, and C. Kumar, "Operation and control of smart transformer in meshed and hybrid grids," *IEEE Ind. Electron. Mag.*, DOI [10.1109/MIE.2020.3005357](https://doi.org/10.1109/MIE.2020.3005357), pp. 0–0, 2020.

[23] M. Couto, J. P. Lopes, and C. Moreira, "Control strategies for multi-microgrids islanding operation through smart transformers," *Electric Power Systems Research*, vol. 174, DOI <https://doi.org/10.1016/j.epr.2019.105866>, p. 105866, 2019.

[24] D. Das, V. M. Hrishikesan, C. Kumar, and M. Liserre, "Smart transformer-enabled meshed hybrid distribution grid," *IEEE Trans. Ind. Electron.*, vol. 68, DOI [10.1109/TIE.2020.2965489](https://doi.org/10.1109/TIE.2020.2965489), no. 1, pp. 282–292, 2021.

[25] C. Kumar, R. Manojkumar, S. Ganguly, and M. Liserre, "Power loss minimization in smart transformer based meshed hybrid distribution network," in *IECON 2020 The 46th Annu. Conf. IEEE Ind. Electron. Soc.*, DOI [10.1109/IECON43393.2020.9254324](https://doi.org/10.1109/IECON43393.2020.9254324), pp. 1670–1675.

[26] G. De Carne, G. Buticchi, Z. Zou, and M. Liserre, "Reverse power flow control in a st-fed distribution grid," *IEEE Trans. Smart Grid*, vol. 9, DOI [10.1109/TSG.2017.2651147](https://doi.org/10.1109/TSG.2017.2651147), no. 4, pp. 3811–3819, Jul. 2018.

[27] Cigre Task Force C6.04.02, "Benchmark systems for network integration of renewable and distributed energy resources," Tech. Rep., Apr. 2014.

[28] R. Manojkumar, C. Kumar, S. Ganguly, H. B. Gooi, and S. Mekhilef, "Voltage control using smart transformer via dynamic optimal setpoints and limit tolerance in a residential distribution network with pv sources," *IET Gener. Transm. Distrib.*, vol. 14, no. 22, pp. 5143–5151, 2020.

[29] S. Ganguly, "Multi-objective planning for reactive power compensation of radial distribution networks with unified power quality conditioner allocation using particle swarm optimization," *IEEE Trans. Power Syst.*, vol. 29, no. 4, pp. 1801–1810, 2014.

[30] X. Liu, A. Aichhorn, L. Liu, and H. Li, "Coordinated control of distributed energy storage system with tap changer transformers for voltage rise mitigation under high photovoltaic penetration," *IEEE Trans. Smart Grid*, vol. 3, no. 2, pp. 897–906, 2012.

[31] N. B. Roy and D. Das, "Optimal allocation of active and reactive power of dispatchable distributed generators in a droop controlled islanded microgrid considering renewable generation and load demand uncertainties," *Sustain. Energy, Grids Netw.*, vol. 27, DOI <https://doi.org/10.1016/j.segan.2021.100482>, p. 100482, 2021.

[32] z. Yeniay, "Penalty Function Methods for Constrained Optimization with Genetic Algorithms," *Math. Comput. Appl.*, vol. 10, DOI [10.3390/mca10010045](https://doi.org/10.3390/mca10010045), no. 1, pp. 45–56, 2005.

[33] S. Das and S. Mukhopadhyay, "Sensing error minimization for cognitive radio in dynamic environment using death penalty differential evolution based threshold adaptation," in *2016 IEEE Annual India Conference (INDICON)*, DOI [10.1109/INDICON.2016.7838865](https://doi.org/10.1109/INDICON.2016.7838865), pp. 1–6, 2016.

[34] X.-S. Yang, "Chapter 6 - genetic algorithms," in *Nature-Inspired Optimization Algorithms (Second Edition)*, second edition ed., X.-S. Yang, Ed., pp. 91–100. Academic Press, 2021.

[35] K. Gaur, H. Kumar, R. P. K. Agarwal, K. V. S. Baba, and S. K. Soonee, "Analysing the electricity demand pattern," in *2016 Nat. Power Syst. Conf. (NPSC)*, pp. 1–6.

[36] V. K. Agrawal, A. Khemka, K. Manoharan, D. Jain, and S. Mukhopadhyay, "Wind-solar hybrid system – an innovative and smart approach to augment renewable generation and moderate variability to the grid," in *2016 IEEE 7th Power India Int. Conf. (PIICON)*, DOI [10.1109/POWERI.2016.8077152](https://doi.org/10.1109/POWERI.2016.8077152), pp. 1–5.

[37] Economics Division Central Electricity Regulatory Commission, "Report on short-term power market in india: 2018-19." [Online]. Available: http://www.cercind.gov.in/2019/market_monitoring/Annual%20Report%202018-19.pdf

- [38] Y. Hong and M. Wu, "Markov model-based energy storage system planning in power systems," *IEEE Syst. J.*, vol. 13, DOI 10.1109/JSYST.2019.2900081, no. 4, pp. 4313–4323, 2019.
- [39] X. Liu, L. Li, Z. Li, X. Chen, T. Fernando, H. H.-C. Iu, and G. He, "Event-Trigger Particle Filter for Smart Grids With Limited Communication Bandwidth Infrastructure," *IEEE Trans. Smart Grid*, vol. 9, DOI 10.1109/TSG.2017.2728687, no. 6, pp. 6918–6928, 2018.
- [40] F. Etedadi Aliabadi, K. Agbossou, S. Kelouwani, N. Henao, and S. S. Hosseini, "Coordination of Smart Home Energy Management Systems in Neighborhood Areas: A Systematic Review," *IEEE Access*, vol. 9, DOI 10.1109/ACCESS.2021.3061995, pp. 36 417–36 443, 2021.



CHANDAN KUMAR (Senior Member, IEEE) received the B.Sc. degree from the Muzaffarpur Institute of Technology, Muzaffarpur, India, in 2009, the M.Tech. degree from the National Institute of Technology, Trichy, India, in 2011, and the Ph.D. degree from the Indian Institute of Technology Madras, Chennai, India, in 2014, all in electrical engineering.

Since 2015, he has been an Assistant Professor with the Electronics and Electrical Engineering

Department, Indian Institute of Technology Guwahati, Guwahati, India. During 2016 to 2017, he was an Alexander von Humboldt Research Fellow with the Chair of Power Electronics, University of Kiel, Kiel, Germany. His research interests include power electronics application in power system, power quality, and renewable energy. He is serving as Associate Editor of IEEE Open Journal of Power Electronics, IEEE Open Journal of the Industrial Electronics Society (OJIES), and IEEE Access Journal.



RAMPELLI MANOJKUMAR (Student Member, IEEE) received the B.E. degree in electrical and electronics engineering from Vasavi College of Engineering, Hyderabad, India, in 2013, and the M.Tech. degree in power and energy systems from the National Institute of Technology Karnataka, Surathkal, India, in 2015.

He is currently working toward the doctoral degree with the Department of Electronics and Electrical Engineering, Indian Institute of Tech-

nology Guwahati, Guwahati, India. His research interests include optimal energy management using batteries, power electronics applications in modern distribution systems, hybrid ac/dc distribution systems and smart grid.



SANJIB GANGULY (Senior Member, IEEE) was born in 1981 in India. He received the B.E. and M.E. degrees in electrical engineering from Indian Institute of Engineering Science and Technology, Shibpur, India and Jadavpur University, India in 2003 and 2006, respectively. He received the Ph.D degree from Indian Institute of Technology Kharagpur, India in 2011.

He is presently working as Associate Professor in the Department of Electronics and Electrical

Engineering in Indian Institute of Technology Guwahati, India. His research interest includes power system operation and planning, custom power devices, hybrid energy system, and evolutionary algorithms.



MARCO LISERRE (Fellow, IEEE) received the M.Sc. and Ph.D. degrees in electrical engineering from Bari Polytechnic, Bari, Italy, in 1998 and 2002, respectively. He has been an Associate Professor with Bari Polytechnic and, from 2012, a Professor in reliable power electronics with Aalborg University, Denmark. Since 2013, he has been a Full Professor and holds the Chair of Power Electronics with Kiel University, Kiel, Germany. He has authored or coauthored 500 technical pa-

pers (1/3 of them in international peer reviewed journals) and one book. These works have received more than 35000 citations.

Dr. Liserre is listed in ISI Thomson report "The worlds most influential scientific minds" from 2014. He has been awarded with an ERC Consolidator Grant for the project The Highly Efficient And Reliable smart Transformer (HEART), a new Heart for the Electric Distribution System. He is a member of IAS, PELS, PES, and IES, and has been serving all these societies in different capacities. He was the recipient of the IES 2009 Early Career Award, the IES 2011 Anthony J. Hornfeck Service Award, the 2014 Dr. Bimal Bose Energy Systems Award, the 2011 Industrial Electronics Magazine Best Paper Award, and the Third Prize Paper Award by the Industrial Power Converter Committee at ECCE 2012, 2012, 2017 IEEE PELS Sustainable Energy Systems Technical Achievement Award, and the 2018 IEEE-IES Mittelmann Achievement Award.

...